

Reconfigurable Photonic Integrated Reservoir for Different Baud-Rate PAM-4 Signal Recognition

Kailai Liu¹, Ying Zhu^{1,2,*}, Siyao Chang², Ming Lei², Chao Yang¹, Qiansheng Wang², Xi Xiao^{1,2,3}

¹State Key Laboratory of Optical Communication Technologies and Networks, China Information and Communication Technologies Group Corporation (CICT), Wuhan 30074, China

²National Information Optoelectronics Innovation Center, China Information and Communication Technologies Group Corporation (CICT), Wuhan 430074, China

³Peng Cheng Laboratory, Shenzhen 518055, China

*zhuying@wri.com.cn

Abstract: A reconfigurable photonic integrated reservoir based on Mach-Zehnder Interferometer nodes is proposed. It can be programmed to adapt to different baud-rate IMDD systems for PAM-4 signal recognition. The photonic reservoir-based receivers can achieve a lower bit error rate and consume $0.5 \times$ power compared to their conventional electronic counterparts.

© 2024 The Author(s)

1. Introduction

Artificial Intelligence (AI), including Foundation Models like GPT-3 and GPT-4, has made significant breakthroughs. These applications necessitate substantial computing power, which is primarily facilitated through the collaborative effort of numerous high-performance servers and specialized hardware accelerators in data centers. Currently, data transmission in data centers is mainly supported by the Intensity Modulated Direct Detection (IMDD) systems, which are low in complexity and cost-effective. These systems employ tapped delay line filters (TDL) for signal equalization and compensation [1]. However, the exponential growth in computing power requirements demands higher data throughput and increased signal processing rate. Consequently, there is a need for complicated high-speed CMOS circuit design and a more intricate equalization process at the receiver's analog-to-digital converter (ADC) and digital signal processing (DSP).

The optical or photonic reservoir network, as a novel recursive neural network structure, can process and memory high-speed signals in the analog optical domain, effectively conserving computational resources in the electronic circuits and well-suited for hardware implementation [2,3]. A delay-based optical storage layer structure proposed in [4] enables equalization for 112 Gb/s PAM-4 signals in 5.5 KM fibers. However, the structure, including a reservoir semiconductor laser, an attenuator, a high bandwidth photodetector (PD), and a high-speed ADC, is challenging in integration. Another integrable spatial reservoir structure in [5,6] has experimentally equalized a 32 Gb/s OOK signal, which outperforms its electronic counterpart. However, this fixed-structure reservoir is only suitable for signals at a specific baud rate, and its performance degrades when applied to systems with other rates.

Here, we propose a spatial photonic integrated reservoir structure composed of waveguides and Mach-Zehnder Interferometer (MZI) nodes, which can be integrated using silicon photonics technology and is amenable to real-time reconfiguration. By programming the phase shifters in the MZI nodes, the reservoir can adjust its inner connection delay to adapt to different data rates. We set up a simulation platform for the reservoir structure and apply it to process PAM-4 signals from real IMDD systems with baud rates ranging from 30G to 60G spanning 2.5 km. Lower BERs than the TDL are obtained even when the number of reservoir outputs is only about 1/4 of the tap number in the TDL. Since the reservoir can memory link information, the working frequency of the reservoir-based receiver can work only half of the frequency of the TDL-based receiver, reducing the overall power consumption of ADCs by 53.0%.

2. Reconfigurable Photonic Integrated Reservoir

We propose an $M \times M$ spiral MZI mesh as in Fig. 1(a), in which there are M -column and M -row MZI nodes connected with a spiral waveguide mesh. The waveguide delay between neighboring MZI nodes is L . The spiral reservoir structure incorporates $2M$ input nodes distributed along the mesh edges. Optical signals are input to the reservoir in parallel after undergoing equal splitting. By programming the phase shift difference $\Delta\theta = 0, \pi/4, \pi/2$ between the upper and lower arms of the MZIs, the MZI nodes can implement cross, mixing, or parallel configurations for optical signals as in Fig. 1(b). The phase difference $\Delta\theta$ at the four corners of the mesh is set to parallel states ($\Delta\theta = \pi/2$), allowing optical signals at the corners to complete a full 90° rotation. When the phase shift difference $\Delta\theta$ is $\pi/4$, the MZI mixes the two input signals. If the MZI $\Delta\theta = 0$, the two optical input signals pass through the MZI without interference. Optical signals within the mesh undergo counterclockwise rotation and mixing along the waveguides and MZI nodes. Earlier signals gradually attenuate over time, while new signals continuously enter, forming a photonic reservoir structure.

According to the observation in [7] the reservoir with a waveguide delay l between two mixing nodes can achieve optimal performance for signals with a symbol period of $2l$ (baud-rate $B = \frac{1}{2l}$). By programming the corresponding MZI nodes to cross and mixing states, the waveguide delay l between two mixing nodes can be adjusted to adapt to different baud-rate IMDD systems. For instance, if we set all the MZI nodes except those at the four corners to mixing states and the waveguide delay l between two mixing nodes is L , the reservoir is suitable for the signal with a symbol period of $2L$ ($B_1 = \frac{1}{2L}$). If each alternate MZI node in the mesh except those at the four corners is set to mixing states

and the other one set to cross state, leading to a waveguide delay of $2L$ between the two mixing nodes, the reservoir is suitable for signals with a symbol period of $4L(B_2 = \frac{1}{4L} = \frac{1}{2}B_1)$. Generally, we can set $\Delta\theta$ to zero at every K MZI nodes, which corresponds to K times the waveguide delay, thereby adapting it to the $B_k = \frac{1}{K}B_1$ as in Fig. 1(c).

Regarding the output section of the reservoir, we implement an electrical readout strategy. The two outputs from each MZI node, totaling $2M^2$, are sampled by ADCs after being detected by PDs. The ADC power consumption, dominant in the receiver power consumption, is proportional to v^2f , i.e., $P \propto v^2f$, where v is the supply voltage and f is the clock frequency. Under a specific process technology, $v \propto f$, resulting in the power consumption of ADCs being roughly cubic to frequency [8]. Due to reservoir memory characteristics, it is possible to obtain N adjacent symbols by fitting N different regression models to a single readout. This enables the sampling rate at the receiving end to be lower than the baud rate at the transmitting end. The previously required high-speed ADC can be replaced by N ADCs with much lower sampling rates, thereby, reducing the power consumption and circuit complexity for receivers. The quantized $2M^2$ data after ADCs are weighted and summed in DSPs for symbol recognition. The weights are primarily trained utilizing a linear regression algorithm. The labels used for training are PAM-4 data streams. To reduce the costs of ADCs and DSPs, we develop an automatic training method. This method involves penalizing the weight absolute values during training, removing the weights whose absolute values are smaller than a threshold, and retuning the left weights. As a result, only a subset of outputs is necessary, leading to a reduction in the number of used ADCs and the amount of computation in DSPs.

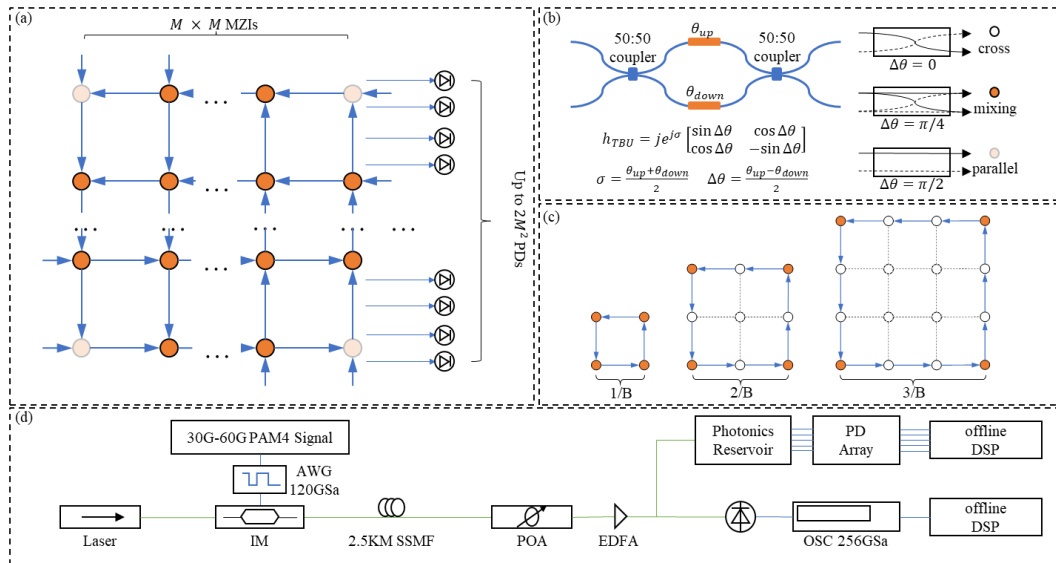


Fig. 1. Reconfigurable photonic integrated reservoir. (a) An $M \times M$ -sized reservoir and the PD array. (b) The MZI structure and its transmission matrix, with different output configurations and corresponding node colors for varying values of $\Delta\theta$ on the right. (c) Increasing the interconnect delay by setting $\Delta\theta$ to zero for differently spaced MZIs. (d) IMDD system used for the experiment. IM: intensity modulator, AWG: arbitrary wave generator, SSMF: Standard single mode fiber, POA: Programmable optical attenuation, EDFA: erbium-doped fiber amplifier, OSC: oscilloscope

3. Results and Discussion

We conducted numerical simulations on the photonic reservoir structure with dimensions of 17×17 . PAM-4 signals were generated and recorded by the real IMDD system shown in Fig. 1(d). Data at the receiving end were firstly mapped equivalently back to the optical field and then input from 34 input points in the reservoir. The reservoir outputs were weighted in the electronic domain. To demonstrate the necessity for waveguide delay programming, we changed the waveguide delay $l = \frac{1}{4B}, \frac{2}{4B}, \frac{3}{4B}, \frac{4}{4B}$ for 60 GBaud PAM-4 signals. Fig. 2(a) presents the reservoir achieves optimal BER under different received optical power when the waveguide delay is half of the symbol period.

To demonstrate the effectiveness of the reconfigurable photonic reservoir for PAM-4 signal processing under different baud rates, we configured the waveguide delay l to be half of the symbol period at a 120GBaud rate. By setting $\Delta\theta$ to zero for different spaced MZIs, we were able to multiply the waveguide delay of this reservoir by 2, 3, or 4, respectively, to adapt it to the 60G, 40G, and 30G baud-rate signals. After reconfiguration, the reservoir structures were tailored into 5×5 meshes, which means that a total of 50 outputs are available for signal recognition. With the automatic training method, only 30 outputs are selected for linear regression. Fig. 2(b) presents the reconfigured reservoirs can obtain a lower BER than the 117-tap TDL method under different baud rates.

Besides, the structure suggests that a practical chip requires only 30 PDs and ADCs are required, and the DSP needs to process 30 data points at a time. Since a low sampling rate can lead to a reduction in power consumption and

circuit complexity, we compare the performance of the reservoir with one linear regression to recover one symbol working at the symbol baud rate and one with two linear regressions to recover two adjacent symbols under half of the baud rate. The latter can be implemented using two parallel-processing DSPs, and then the recovered symbols are concatenated to reconstruct the original data stream. Fig. 2(c) shows the BER of the structures under the same baud rate and half of the baud rate. The dashed lines representing the half-sampling strategy result in slightly higher BER only in specific scenarios. Therefore, it is feasible of employing the half-sampling strategy of processing signals with two parallel DSPs at a reduced sampling rate.

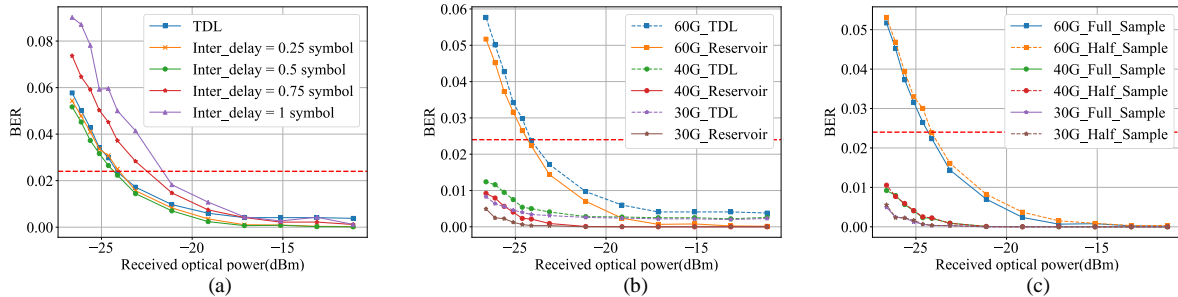


Fig. 2. BER vs. received optical power. (a) BER of 60Gbaud rate PAM-4 signals obtained from photonic reservoir with different interconnect delays. (b) BER of 30G, 40G and 60G baud rate PAM-4 signals obtained from corresponding reconfigured photonic reservoirs. (c) BER of 30G, 40G, and 60G baud rate PAM-4 signals obtained from reservoir processed at full sample (sample rate = baud rate) and half sample (sample rate = 1/2 baud rate).

As mentioned previously, the photonic reservoir has the potential to reduce the hardware cost. Thus, we compare the hardware resources between the photonic reservoir and TDL filter system as in Table 1 under the assumption that the manufacturing process for the ADCs and DSPs and the symbol recognition speed are the same. According to the relation between power and working frequency, although the photonic reservoir uses 30 photodetectors and ADCs, the overall power consumption is approximately 0.47 times that of the TDL filter system due to its required sampling rate being only 0.25 times that of the TDL. Similarly, employing two DSPs with half of the rate in the one DSP strategy can further reduce power consumption to 0.25 times.

Table 1. Hardware Resource Consumption Comparison

Method	No. of PDs	Sampling Rate	ADC Power	No. of DSPs	DSP speed	DSP Power
TDL	1	$>2 \times$ Baud Rate	1	1	Baud Rate	1
PR	30	$1/2 \times$ Baud Rate	0.47	2	$1/2 \times$ Baud Rate	0.25

4. Conclusion

We propose a reconfigurable photonic integrated reservoir based on MZI nodes. We have successfully simulated that the reservoir can be programmed to adapt to recognize PAM-4 signals at the rate from 30G to 60G baud over a 2.5 km optical fiber with lower BER than that of a 117-tap TDL filter. The performance is achieved using only 30 parallel photodetectors and ADCs and two DSPs operating at half the baud rate. Furthermore, the power consumption of the ADC and DSP can approximate $0.47 \times$ and $0.25 \times$, respectively, to that of the TDL structure. This method exhibits a great potential for optical interconnect scenarios in data centers, providing substantial hardware resource savings. Its prospect is especially encouraging due to the fast progress of AI Foundation models in high-speed environments.

This work was supported by the Natural Science Foundation of Hubei Province, China (2023AFB528) and National Natural Science Foundation of China (U21A20454).

References

- [1] X. Zhou, R. Urata, and H. Liu, "Beyond 1 Tb/s intra-data center interconnect technology: IM-DD OR coherent?," *Journal of Lightwave Technology* **38**, 475-484 (2019).
- [2] H. Jaeger, "The "echo state" approach to analysing and training recurrent neural networks-with an erratum note," Bonn, Germany: German National Research Center for Information Technology GMD Technical Report **148**, 13 (2001).
- [3] W. Maass, T. Natschläger, and H. Markram, "Real-time computing without stable states: A new framework for neural computation based on perturbations," *Neural computation* **14**, 2531-2560 (2002).
- [4] A. Argyris, J. Bueno, and I. Fischer, "PAM-4 transmission at 1550 nm using photonic reservoir computing post-processing," *IEEE Access* **7**, 37017-37025 (2019).
- [5] K. Vandoorne, P. Mechet, T. Van Vaerenbergh, M. Fiers, G. Morthier, D. Verstraeten, B. Schrauwen, J. Dambre, and P. Bienstman, "Experimental demonstration of reservoir computing on a silicon photonics chip," *Nature communications* **5**, 3541 (2014).
- [6] S. Sackesyn, C. Ma, J. Dambre, and P. Bienstman, "Experimental realization of integrated photonic reservoir computing for nonlinear fiber distortion compensation," *Optics Express* **29**, 30991-30997 (2021).
- [7] A. Katumba, X. Yin, J. Dambre, and P. Bienstman, "A neuromorphic silicon photonics nonlinear equalizer for optical communications with intensity modulation and direct detection," *Journal of Lightwave Technology* **37**, 2232-2239 (2019).
- [8] M. McCool, J. Reinders, and A. Robison, *Structured parallel programming: patterns for efficient computation* (Elsevier, 2012).